STUDY OF THE ELASTIC SCATTERING OF ^{14}N ON ^{12}C

by

JAMES H. JOHNSON

B. A., University of Northern Colorado, 1972

A MASTER'S THESIS

submitted in partial fulfillment of the

requirements for the degree

MASTER OF SCIENCE

Department of Physics

KANSAS STATE UNIVERSITY
Manhattan, Kansas

1974

Approved by:

John D. Eck

Major Professor

TABLE OF CONTENTS

LIST OF TABLES

TABLES PAGE

LIST OF FIGURES

I. INTRODUCTION

> The grand aim of all science is to cover the greatest number of empirical facts by logical deduction from the smallest number of hypotheses or axioms.
>
> Albert Einstein
> Life, January 9, 1950

In recent years heavy ion nuclear reactions have been studied with increasing vigor. Among the many experiments that one can perform, elastic scattering is the least complicated and one of the most promising. Compared to the sophisticated electronics required by many experiments, elastic scattering is easy to study experimentally and as long as one does not deviate from the optical-model theory the analysis of elastic scattering is straightforward. Although elastic scattering is uncomplicated, a systematic classification of heavy ion elastic scattering cross sections by optical-model parameters would reveal much information. Also, the parameters can be used for more detailed calculations, such as the Distorted Wave Born Approximation calculation of heavy ion transfer reactions. Considering both the merit and the simplicity of elastic scattering experiments, they seem to be a reasonable first step to an understanding of nuclear heavy ion interactions.

Although much work has been carried out on the elastic scattering of identical nuclei, such as $^{16}O + ^{16}O$, $^{12}C + ^{12}C$ and $^{14}N + ^{14}N$, there has been relatively little work done in this mass region ($A \approx 16$) on reactions where the projectile differs from the target nucleus. Essentially three types of elastic scattering cross sections for identical

particles have been reported in the literature[1]. As will be seen in figure 12, the $^{12}C + ^{12}C$ excitation function is observed to have, in general, random narrow structures of one MeV width. The $^{16}O + ^{16}O$ elastic scattering cross section has more evenly spaced structures of two to three MeV width superimposed on which are narrower structures of about .3 MeV width. Together these exemplify what has been termed intermediate structure. In contrast to these types of excitation functions the $^{14}N + ^{14}N$ elastic scattering cross section is smoothly varying and shows only gross structures of three to five MeV width.[2] It would be interesting to see how the scattering of nonidentical nuclei compares with the observations of identical nuclei scattering. In this dissertation, we report on the measurement of the elastic scattering of $^{14}N + ^{12}C$ for energies near the Coulomb barrier.

The $^{12}C + ^{13}C$ elastic scattering cross section has been reported to show resonant structure in this energy range.[3] Although it has been predicted[4] that the $^{14}N + ^{12}C$ cross section will not show these structures it is of interest to study this hypothesis. It has been assumed that the optical model parameters which describe the $^{14}N + ^{12}C$ are an average of the parameters which describe the $^{14}N + ^{14}N$ and the $^{12}C + ^{12}C$ elastic scattering.[5] This assumption is investigated in the present work by an optical model analysis of the measured $^{14}N + ^{12}C$ elastic scattering cross sections.

To investigate the elastic scattering of $^{14}N + ^{12}C$ we measured angular distributions at ^{14}N bombarding energies of 20.0, 21.0 and 23.5 MeV in the angular range from $\Theta_{cm} = 20°$ to 120°. Excitation functions

were measured at θ_{lab} = 25°, 35°, 45°, and 55° in the bombarding energy range from 15 to 24.8 MeV. Both fine and coarse energy resolution excitation functions were measured. A detailed study of the optical model parameters which best describe the measured cross sections was performed and these results are compared to the results of similar heavy ion scattering measurements in this mass region.

II. EXPERIMENT

> She makes me wash, they comb me all to thunder--the widder eats by a bell; she goes to bed by a bell; she gets up by a bell--everything's so awful reg'lar a body can't stand it.
>
> Mark Twain
> The Adventures of Tom Sawyer

A. Beam

The ^{14}N beam was obtained by introducing methane and nitrogen gas into a diode ion source. The gases were transformed to a plasma by a 110 amp arc. The CN^- ions produced in the source were accelerated to the terminal of the Kansas State University 12 MeV Model EN Tandem Van de Graaff accelerator. At the terminal, foils were used to strip the CN^- ions and ^{14}N was then accelerated in either a 3+ or 4+ charge state. The charge state 3+ was used for the laboratory energy region 15 to 19.5 MeV and the charge state 4+ for the laboratory energy region 19.5 to 24.8 MeV. After passing through the accelerator a series of bending magnets was used to select the desired energy and to direct the beam to the target chamber.

B. Target Chamber

The target chamber used was constructed of stainless steel[6] and consisted of beam collimators, a target holder, a Faraday cup and three concentric rings on which up to eight particle detectors were placed. The target holder allowed selection of up to five targets without letting the chamber up to atmospheric pressure. The three concentric rings allowed external selection of the desired angle between the beam and

the detectors. The detector collimators consisted to two tantalum plates each with rectangular apertures of 9.5 mm by 1.5 mm placed 4.5 cm apart and 20 cm from the target, insuring an angular resolution of less than 1°. The beam collimators, of radius 1.7 mm, were placed 17 cm apart and 40 cm from the targets. This insured that only a small region of the target was bombarded. A Faraday cup was used to monitor the charge collected in order to determine a relative measure of the number of particles passing through the target.

C. Targets

40 $\mu g/cm^2$ and 10 $\mu g/cm^2$ self supporting carbon targets were used. The carbon foils for these targets were commercially obtained and placed on target frames constructed so that an area of .5 cm radius was bare foil. The 40 $\mu g/cm^2$ foils were used to obtain coarse resolution data and the 10 $\mu g/cm^2$ foils were used for the fine resolution data. Charge equilibrium of the beam passing through the target is reached after passing through ~ 4 $\mu g/cm^2$ so that the charge measured by the Faraday cup monitoring system is independent, at least for the 40 $\mu g/cm^2$ targets, of the target thickness and the initial charge state. However, the charge measured is dependent on the beam velocity.

D. Electronics

The charge collected on the Faraday cup was integrated by a Brookhaven Instruments Current Integrator. The pulse output of the Current Integrator, whose rate is proportional to the accumulated charge, was counted by a master scaler and was used to control the flow of data from the particle detectors to the analyzer. Pulses from as

many as eight detectors were preamplified, amplified, sorted in a Mixer Router and accumulated in the TMC multichannel analyzer, or in the Nuclear Science Laboratory Digital Equipment Corporation PDP-15 computer. In both cases, the spectra were distributed over 512 channels when eight detectors were used and over 1024 channels when four or two detectors were used. The spectra were then stored on magnetic tapes.

III. DATA ACQUISITION

> Science is built up with facts, as a house is with stones. But a collection of facts is no more a science than a heap of stones is a house.
>
> Jules Henri Poincarè
> La Science et l'Hypothèse

A. Angular Distributions

Angular distributions were measured with 40 $\mu g/cm^2$ targets in angular steps of 2.5° from θ_{lab} = 10° to 45° which corresponds to θ_{cm} = 20° to 120°. Knowing that the optical model parameters are least sensitive to low energy cross sections, we measured the angular distributions at bombarding energies of 20.0, 21.0 and 23.5 MeV.

A typical spectrum is shown in Figure 1. The yields, Y, or areas under the peaks were extracted from the spectra and recorded as a function of energy. The relative normalization of the yield was obtained by monitoring the number of $^{14}N + ^{12}C$ elastic scattering events, Y_m, in a particle detector placed at a fixed angle. Thus the relative yield, Y_r, is

$$Y_r = Y/Y_m.$$

This number is proportional to the absolute cross section, σ. To find the proportionality constant, k, in the equation, $k \cdot Y_r = \sigma$, we divided σ by the Rutherford scattering cross section, σ_r. It was found that this value is approximately constant for angles forward of $\theta_{cm} \simeq 40°$. It was assumed that the scattering cross section

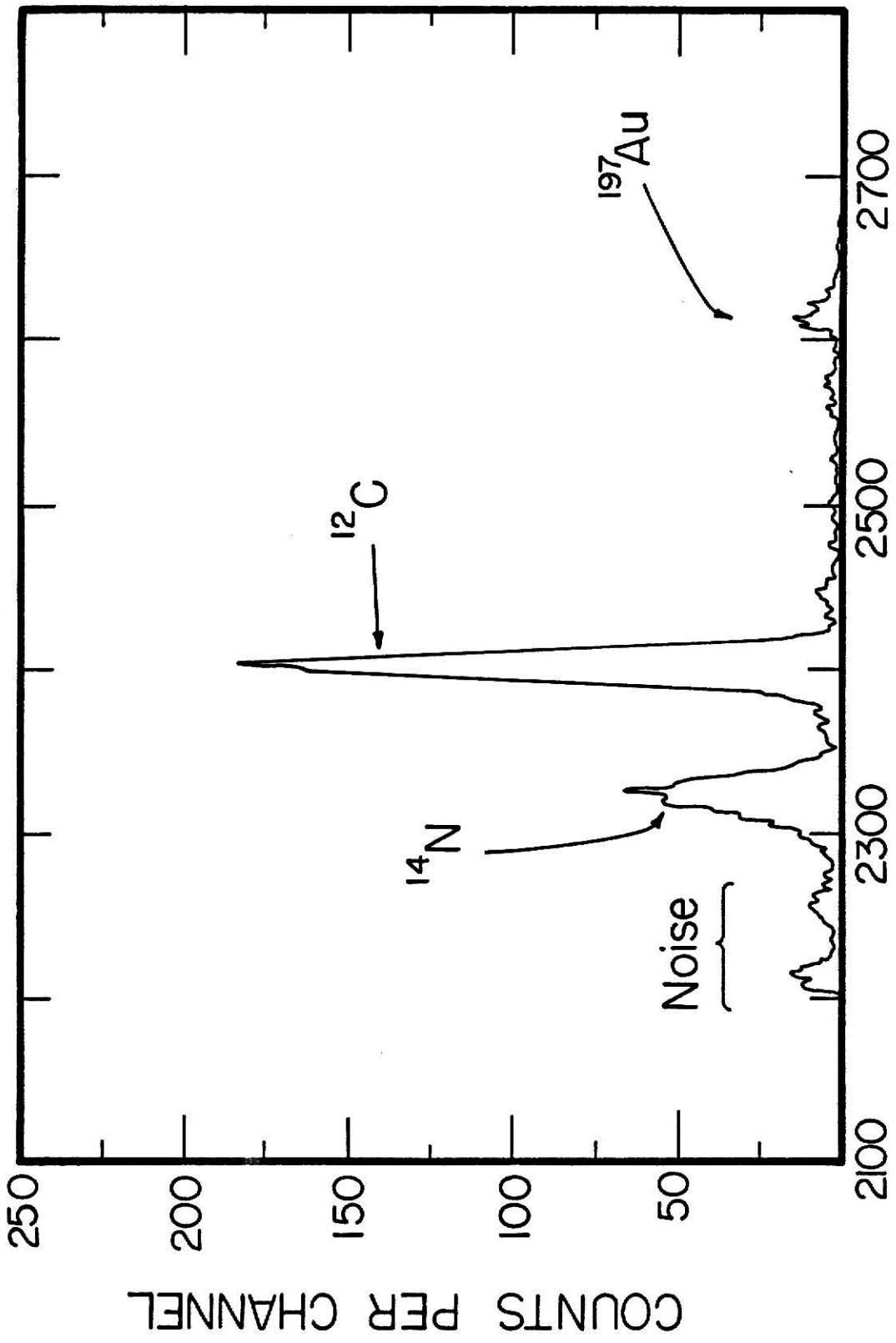

Figure 1. Typical spectrum for ^{14}N + ^{12}C scattering.

at forward angles was pure Rutherford scattering. By setting σ/σ_R equal to one, $\frac{k \cdot Y_r}{\sigma_R} = 1$, the proportionality constant was determined. The angular distributions are shown in Figures 2, 3, and 4.

Since at the backward angles, $\Theta_{cm} > 100°$, the scattered ^{14}N beam is of very low energy, we anticipated trouble distinguishing the particles from the low energy noise. To alleviate this anticipated problem, we determined the yield of the recoiling ^{12}C nuclei at forward angles (high energy carbon) and from kinematics calculated the corresponding angles for the scattered nitrogen nuclei ($\Theta^n_{cm} = 180° - 2 \cdot \Theta^c_{lab}$). By assigning the forward ^{12}C yield to the associated backward ^{14}N we were able to obtain additional data points for $\Theta_{cm} \geq 90°$ and check the σ/σ_R obtained from the detected ^{14}N. There was good agreement between the cross sections calculated by the two different methods. Both cross sections are included in Figures 3 and 4. By either method we were unable, in a reasonable length of time, to get good statistics for backward angles. The statistical error in σ/σ_R for $\Theta_{cm} > 105°$ is as large as 10%. The error in σ/σ_R for $\Theta_{cm} < 100°$ is the size of the dots.

B. Coarse Excitation Functions

Excitation function measurements were performed at $\Theta_{lab} = 25°$, 35° 45° and 55° ($\Theta_{cm} = 51.54°$, 77.0°, 100.6°, and 127.9°) using a thick (40 $\mu g/cm^2$) target. At $\Theta_{lab} = 25°$ only ^{14}N nuclei were detected, at $\Theta_{lab} = 55°$ only ^{12}C nuclei were detected. At $\Theta_{lab} = 35°$ and 45° both $^{14}N + ^{12}C$ Nuclei were detected. By assigning the ^{12}C yield (as described in section A) to the associated ^{14}N we were able to obtain excitation

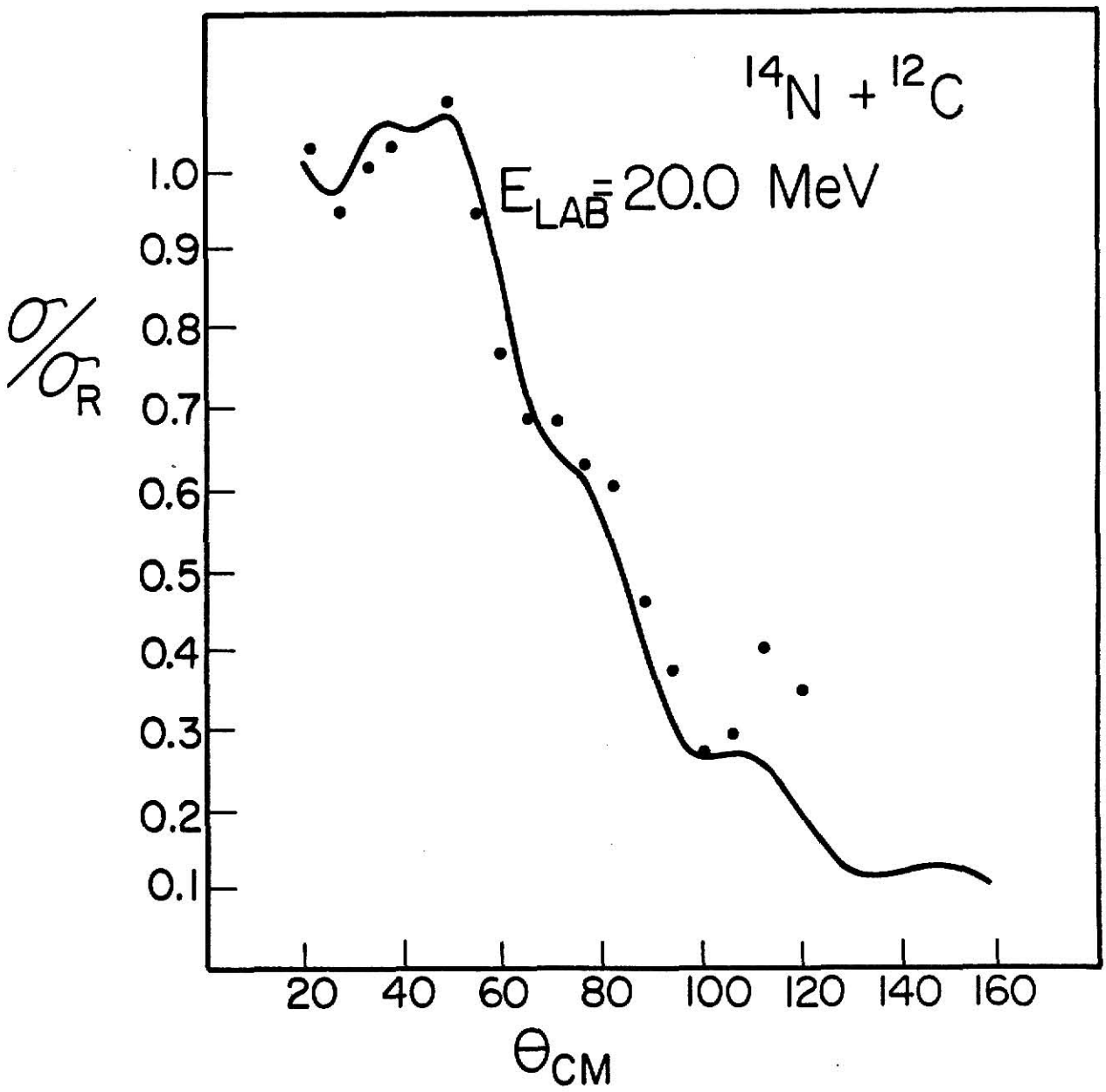

Figure 2. The 20.0 MeV $^{14}N + ^{12}C$ angular distribution.

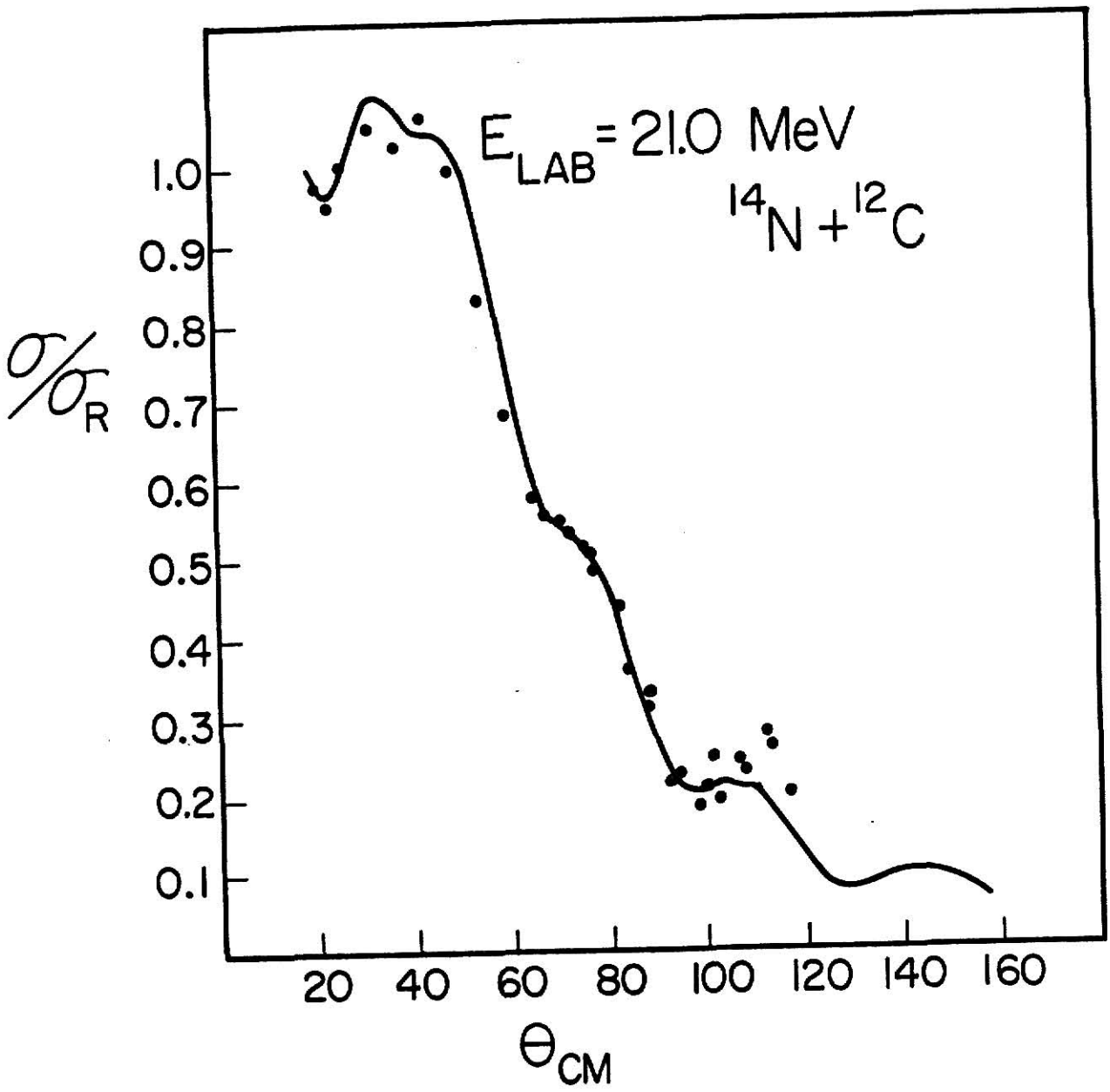

Figure 3. The 21.0 MeV ^{14}N + ^{12}C angular distribution.

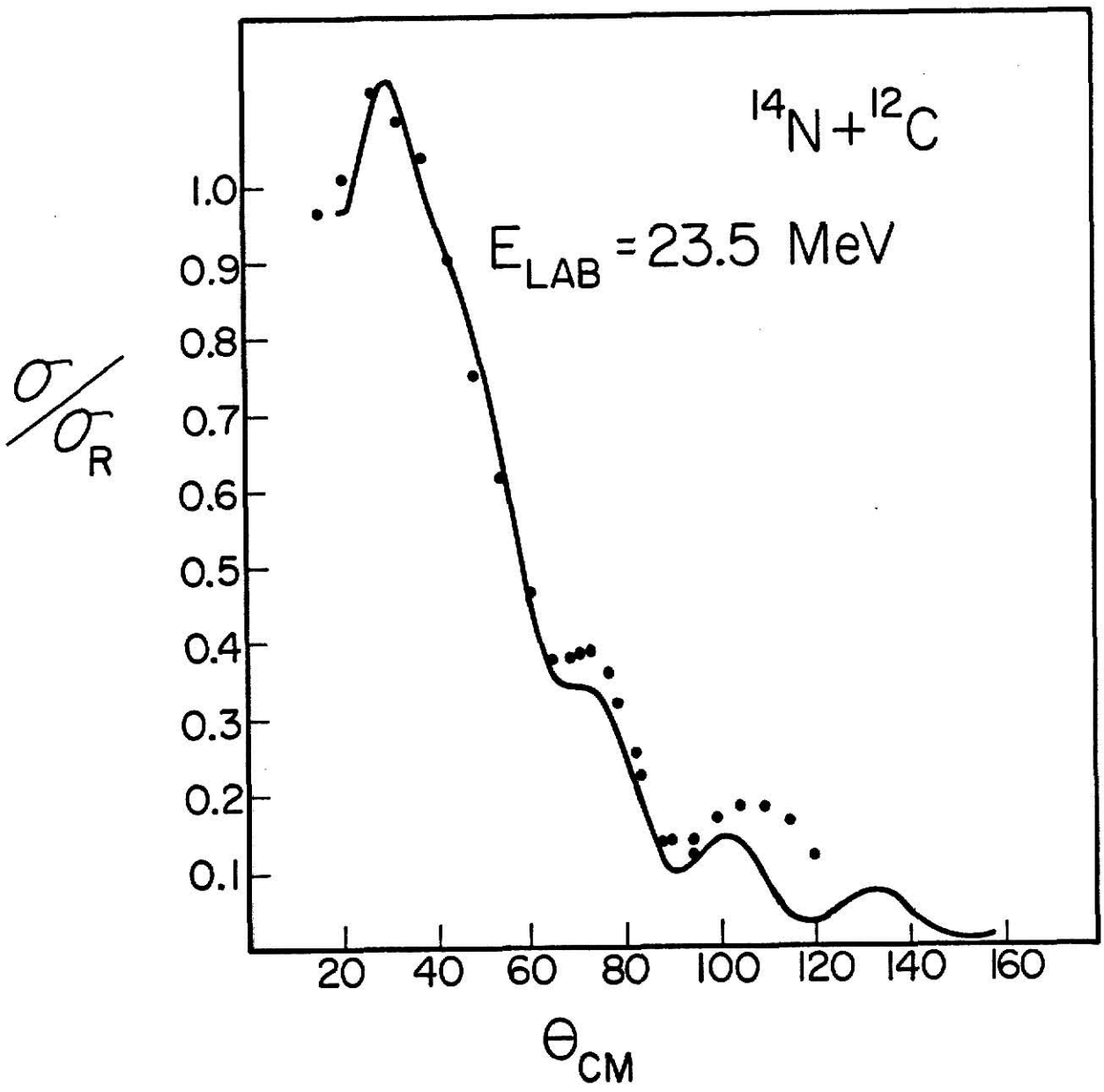

Figure 4. The 23.5 MeV ^{14}N + ^{12}C angular distribution.

functions, which are shown in Figures 5, 6, and 7, at six angles. The energy range measured was 15 to 24.8 MeV with energy steps of 100 keV.

The excitation functions were, in part, measured for a given amount of accumulated charge on the Faraday cup monitoring system. Since the equilibrium charge state of the incident beam varies with energy, a fixed amount of accumulated charge at different energies corresponds to a different number of incident particles and corrections must be made for this effect. Figure 8, Equilibrium Charge States for Nitrogen,[7] gives the probability, p_i, of each charge state, q_i, for a given energy. The average charge, q_{ave}, is the sum of the possible charge states times their probability:

$$q_{ave}(E) = \sum_i p_i(E) q_i(E).$$

To find the energy dependence of q_{ave}, we first calculated the average charge states at several energies (see Figure 9). By the method of least squares, we then fit a parabola to the points and found the relation:

$$q_{ave}(E) = 4.57412 + 0.09224 \cdot E - 0.00092 \cdot E^2.$$

This equation gives an excellent representation, within 1%, of the average charge state as a function of energy for the laboratory energy range 14 to 28 MeV (see Figure 9). By dividing the monitor counts, M, at each energy, by the average charge at that energy the result is proportional to the number of incident particles, N, rather than the charge. Thus, the relation $M(E)/q_{ave}(E) \alpha N$ is independent of energy.

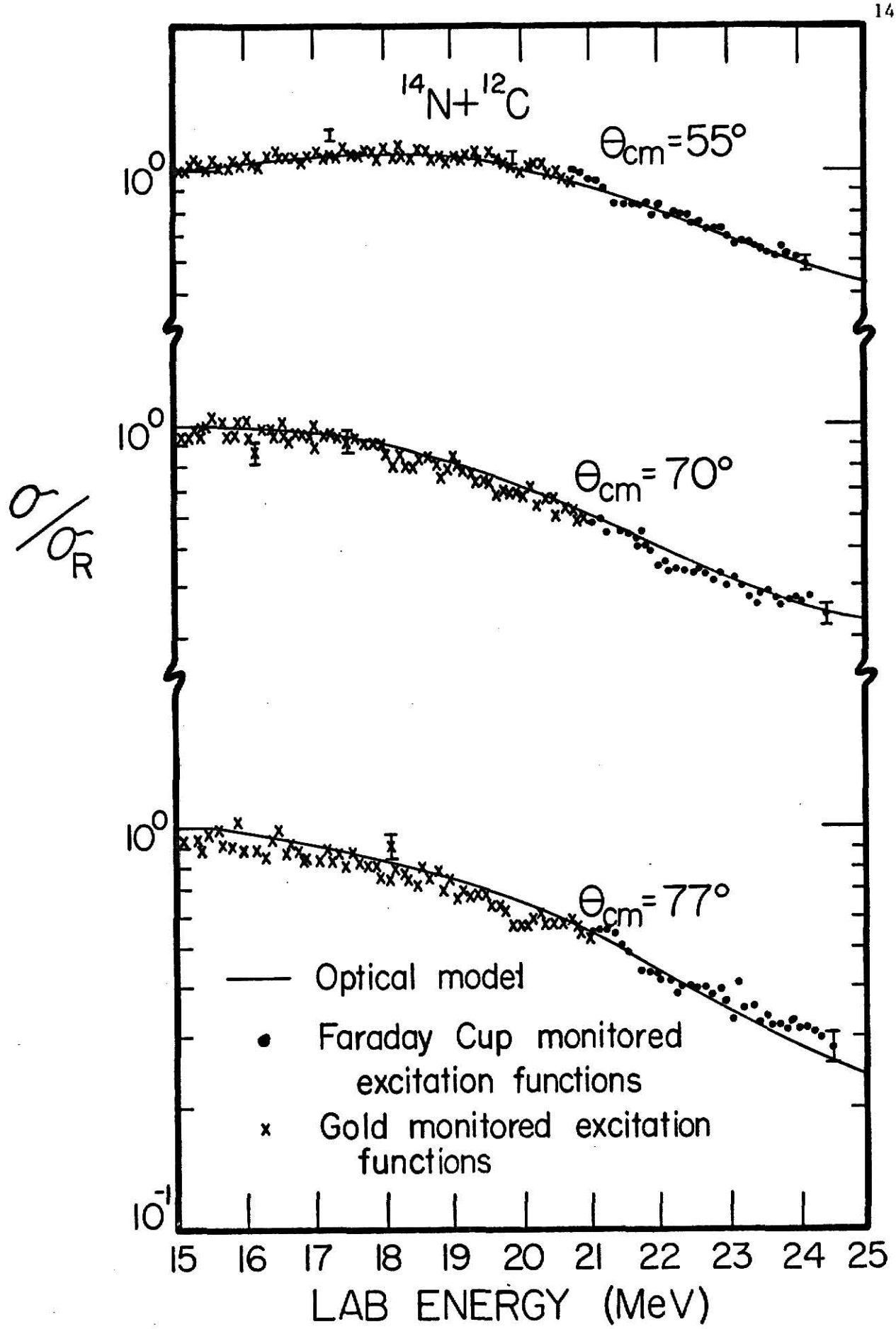

Figure 5. Excitation functions for ^{14}N + ^{12}C scattering.

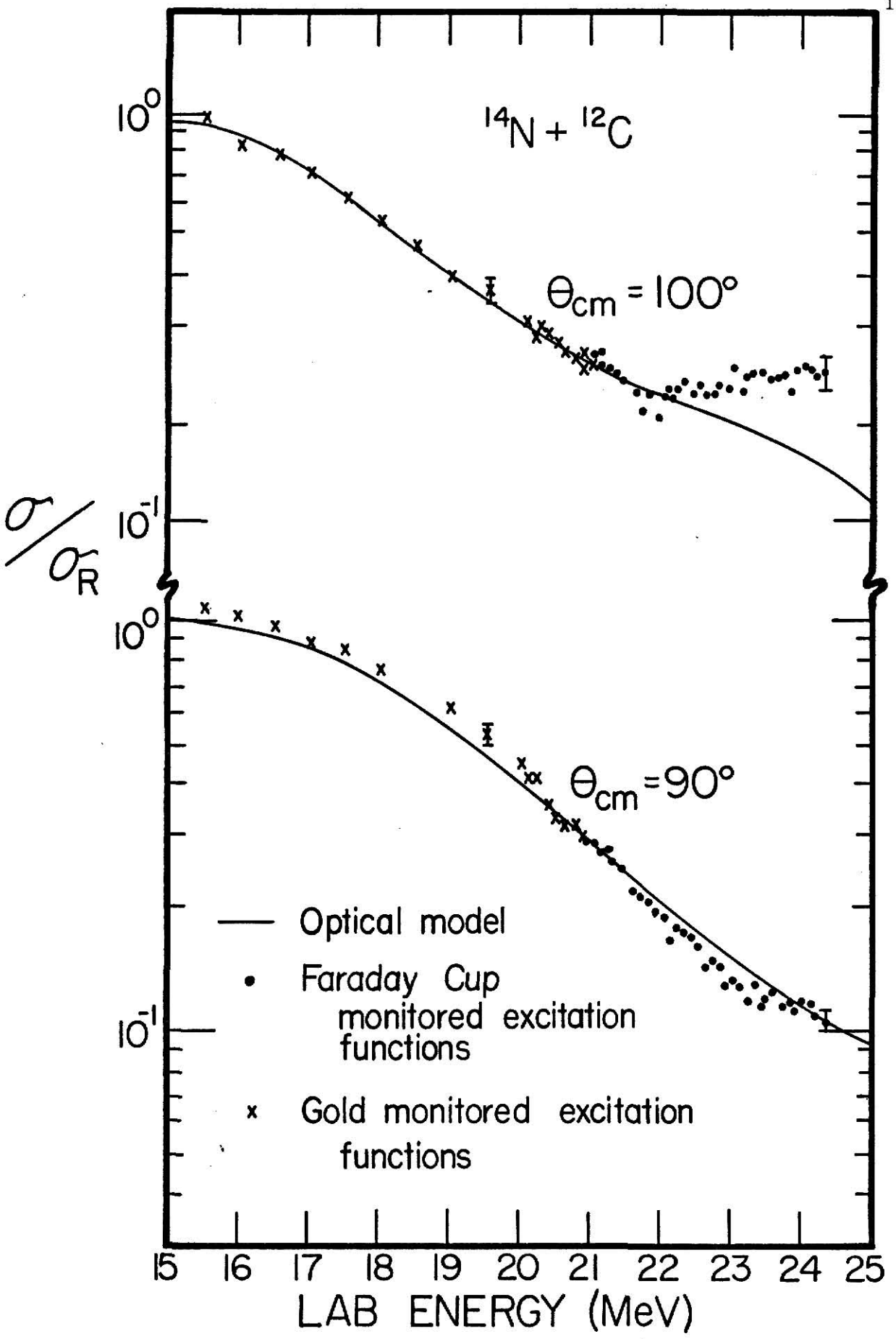

Figure 6. Excitation functions for $^{14}N + ^{12}C$ scattering.

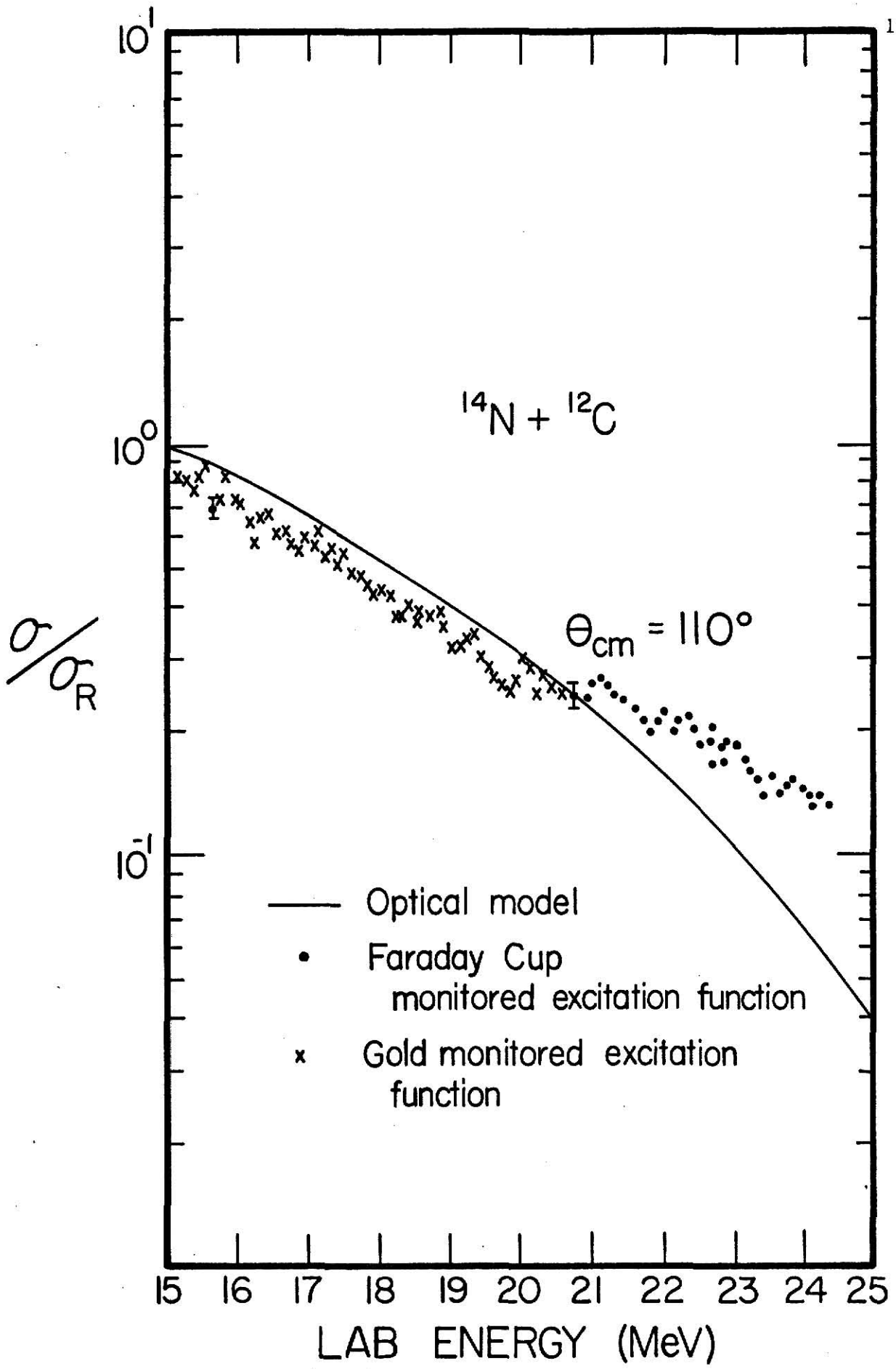

Figure 7. Excitation function for $^{14}N + ^{12}C$ scattering.

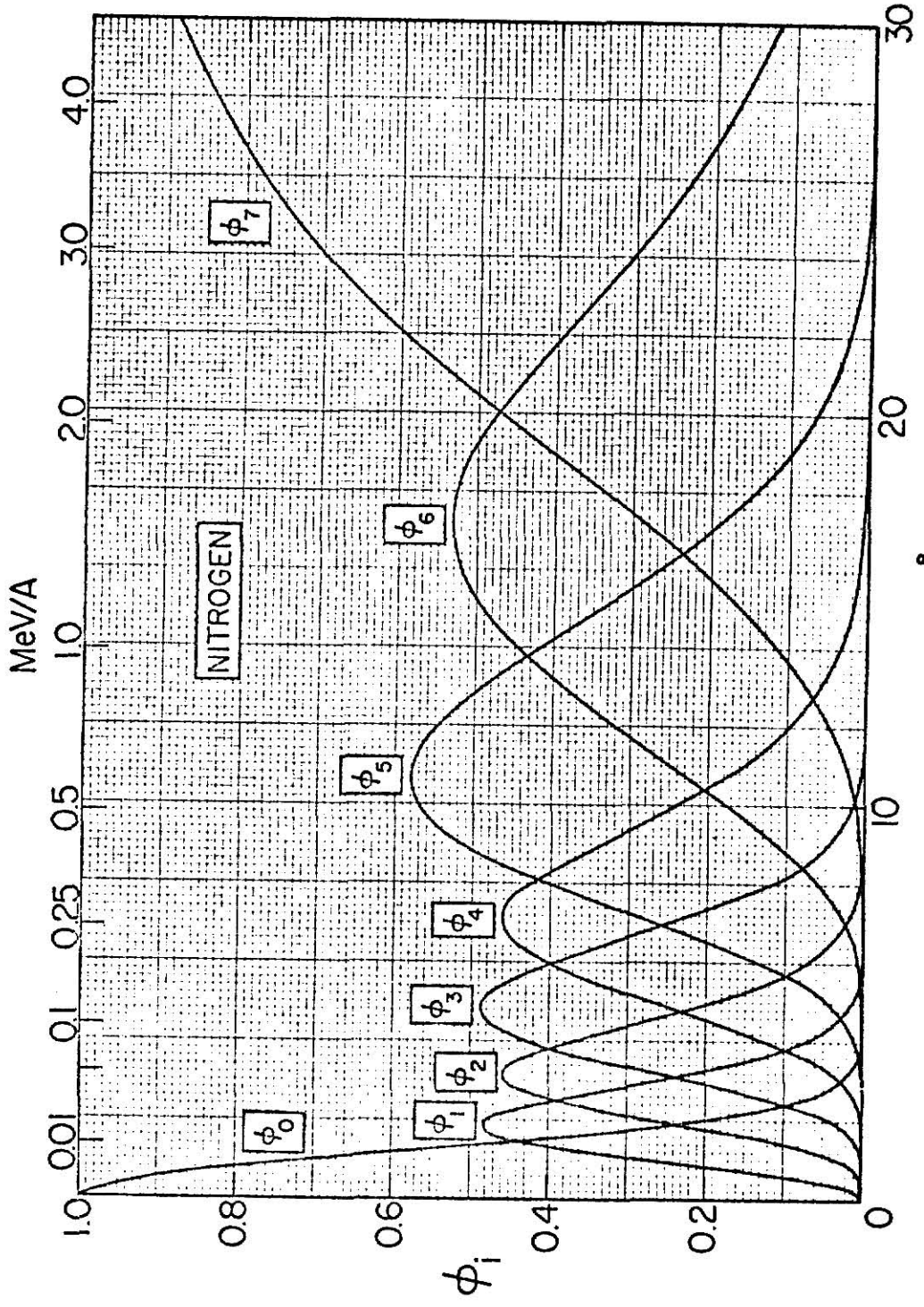

Figure 8. Probability of charge states for nitrogen in solids.

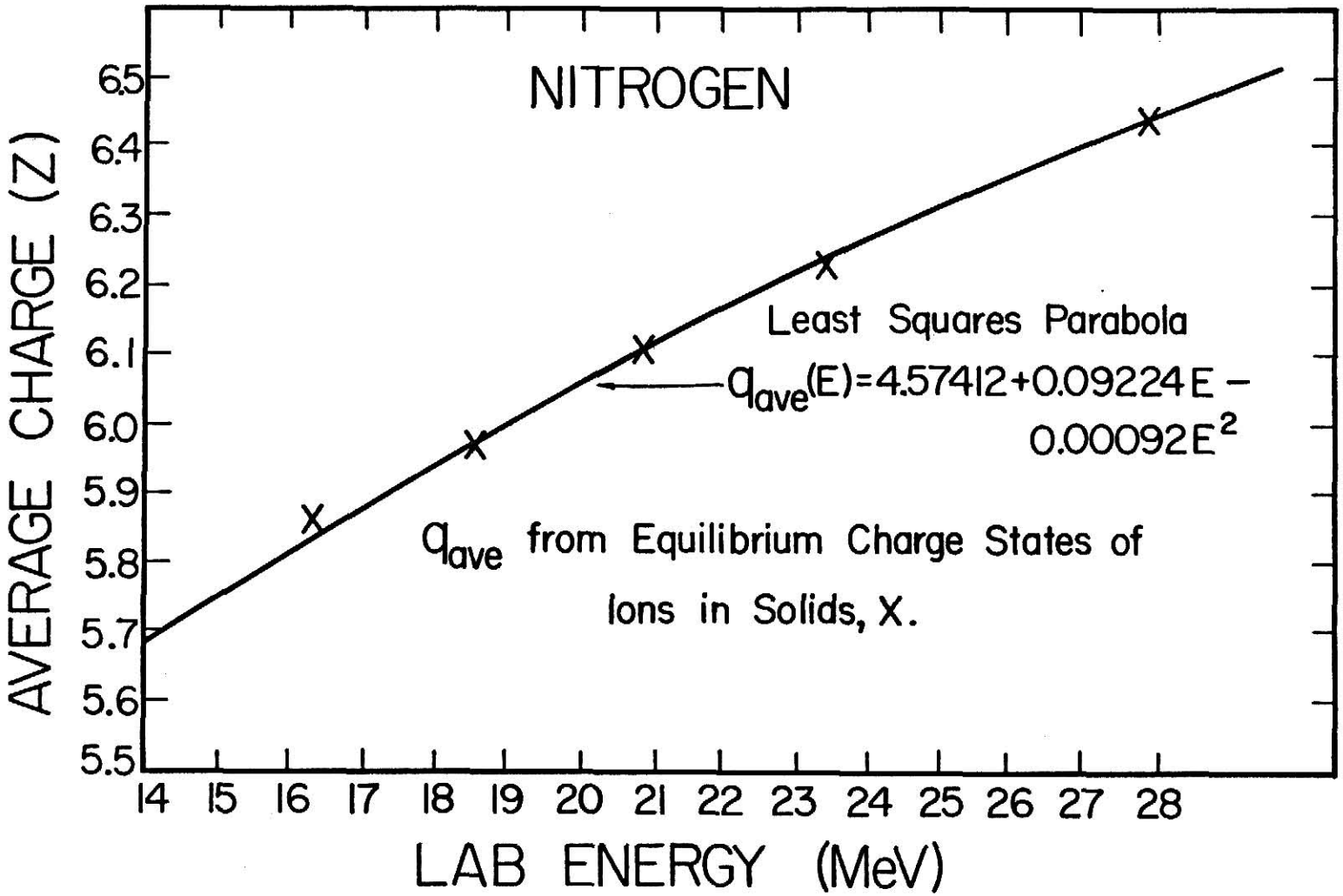

Figure 9. Least squares parabola fit to the average charge state, X, of nitrogen ions in solids.

With this correction the excitation functions were normalized by comparing them to the 21.0 MeV angular distribution (Figure 3).

To verify these excitation functions, we performed the same experiment again, but this time instead of using the Faraday cup monitoring system, we evaporated a trace amount of gold on the carbon targets and normalized to the $^{14}N + ^{197}Au$ elastic scattering peak. Since the $^{14}N + ^{197}Au$ elastic scattering cross section is pure Rutherford scattering over the laboratory energy range 15.0 to 24.8 MeV, the $^{14}N + ^{12}C$ yield divided by the $^{14}N + ^{197}Au$ yield is proportional to σ/σ_R for $^{14}N + ^{12}C$ scattering. Performing this experiment we found that in the laboratory energy region 15 to 20 MeV there was up to a 10% discrepancy between the two different methods. Although we had taken precautions for dead time and had tried to keep the dead time of the Analog to Digital Converter (ADC) below 3%, we found that this dead time was the source of the discrepancy. Above 20 MeV it is very difficult to obtain a large ^{14}N beam and thus we had no dead time problems for laboratory energies above 20 MeV. The agreement between the two cross section measurements for laboratory energies greater than 20 MeV bares this out. For the cross sections taken using a Faraday cup monitoring system we were able to measure the cross section for higher energy. For this reason the excitation functions shown in Figures 5, 6, and 7 are the gold monitored excitation functions up to 21 MeV and the Faraday cup monitored excitation functions for laboratory energies greater than 21.0 MeV.

C. Fine Resolution Excitation Functions

Excitation functions using a thin (10 $\mu g/cm^2$) target were performed in 30 keV steps at angles θ_{lab} = 25°, 45° and 55° over the laboratory energy range 20.0 to 23.8 MeV. Because of the sensitivity of these cross sections to fluctuations in beam energy, incident beam angle, detector angles, and possible uncertainty in the charge equilibrium due to target thickness, we were, to some extent, unable to reproduce the excitation functions. For these reasons, we concentrated on the coarse resolution excitation functions. The fine resolution excitation functions (dots) are compared to those of the coarse (lines) in Figure 10. These excitation functions were not corrected for equlibrium charge distribution effects because of the above mentioned uncertainties. The effect of this is only that the general slope of the curves are slightly less than the equilibrium charge corrected cross sections.

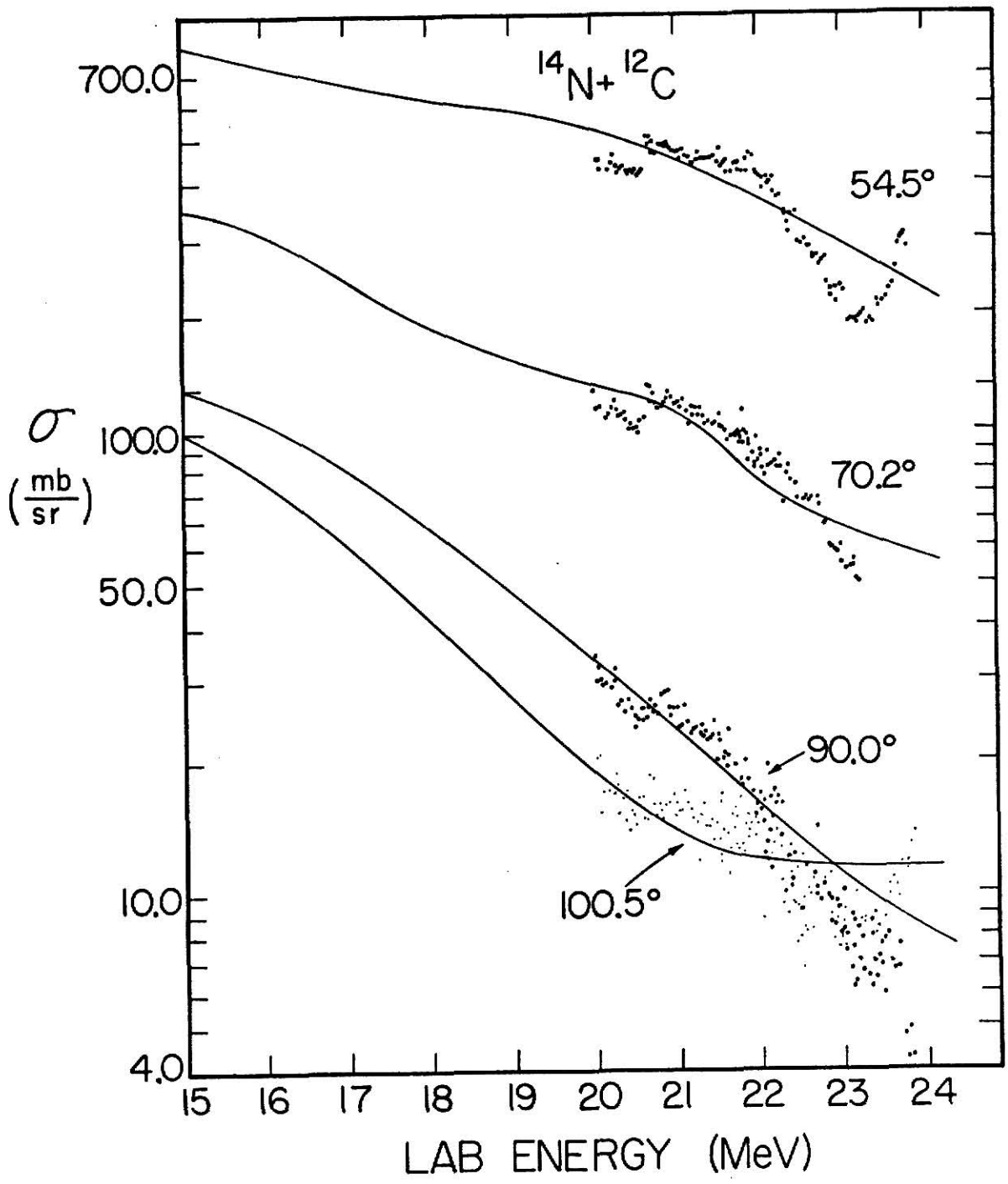

Figure 10. Fine resolution $^{14}N + ^{12}C$ elastic scattering excitation functions. Taken at θ_{cm} = 54.5°, 70.2°, 90.0° and 100.5°.

IV. ANALYSIS

> When you can measure what you are speaking about, and express it in numbers, you know something about it; but when you cannot measure it, when you cannot express it in numbers, your knowledge is of a meager and unsatisfactory kind: It may be the beginning of knowledge, but you have scarcely, in your thoughts, advanced to the stage of science.
>
> William Thomson, Lord Kelvin
> Popular Lectures and Addresses

The measured elastic scattering cross sections were fitted using the optical model. Initially, the angular distributions were fitted and the resulting parameters were then utilized to describe the measured excitation functions. The angular distributions and excitation functions were fitted using computer code SNOOPT2.[8] A four parameter optical model potential was assumed where:

$$U(R) = -(V + iW)\ f(R) + V_c(R)$$

$$f(R) = 1/(1 + \exp(\frac{R - R_o}{a}))$$

$$V_c(R) = \frac{Z_t Z_p}{2R} e^2\ (3 - (\frac{R}{R_o})^2) \qquad R \leq R_o$$

$$= \frac{Z_t Z_p}{R} e^2 \qquad R > R_o$$

$$R_o = r_o(A_t^{1/3} + A_p^{1/3})$$

V is the real potential depth

W is the absorption potential depth

f(R) is the Wood Saxon form factor

R_o is the potential radius

r_o is the potential radius parameter

a is the potential diffuseness

Z_t is the Atomic number of the target

Z_p is the Atomic number of the projectile

e is the electronic charge

A_t is the mass number of the target

A_p is the mass number of the projectile

A. Optical Model and Angular Distributions

The imaginary potential, W, parameterizes the absorption of flux from the elastic scattering channel into various reaction channels. Because the number of open reaction channels increases with increasing bombarding energy it is reasonable to allow W to increase with increasing energy. As seen in Table I this energy dependence is usually of the form

$$W = W_o + .1\ E_{cm}.$$

This would mean that over the energy region in this experiment (E_{lab} = 20.0 to 23.5 MeV) W would change by less than .2 MeV, which affects the optical model cross sections only slightly. Therefore, to find the approximate optical model parameters we searched for the parameters that had the best fit for all three angular distributions. Starting with the parameter set proposed by Von Oertzen[9] to describe $^{12}C + {}^{13}C$ elastic scattering we searched for the minimum χ^2 deviation between experimental angular distributions and theory. The chi-squared value per data point is

$$\chi^2 = \frac{1}{N} \sum_{i=1}^{N} [(\sigma_{th}(i) - \sigma_{exp}(i))/\Delta\sigma_{exp}(i)]^2$$

where σ_{exp} is the experimental cross section, σ_{th} is the optical model cross section evaluated at the same angle as σ_{exp}, $\Delta\sigma_{exp}$ is the statistical error in σ_{exp}, and N is the number of data points. We found that the optical model parameters that best fit all three angular distributions are:

$$V = 96.0 \text{ MeV}$$

$$a = .535 \text{ fm}$$

$$W = 7.0 \text{ MeV}$$

$$R_o = 2.2 \text{ fm.}$$

With these parameters the χ^2 for the three angular distributions at laboratory energies 20.0, 21.0 and 23.5 are 21.1, 6.40 and 13.5, respectively. Figures 2, 3 and 4 show the calculated cross sections and the experimental points. We then searched to find the minimum χ^2 for each individual angular distribution by letting V, a, and W vary, but requiring that V and a remain the same for all three angular distributions. We found that a V of 97.68 MeV, an a of .519 fm and a W of 7.1, 7.43 and 7.83 for the 20.0, 21.0 and 23.5 MeV angular distribution, respectively, were the parameters that fulfilled this requirement. These parameters yielded chi-squares of 20.9, 5.92, and 11.0 for the 20.0, 21.0 and 23.5 MeV angular distribution, respectively. These parameters are listed in Table I with parameters obtained using a similar analysis for nuclei in the same mass region.

There appears to be a large variation in the sets of optical model

System	V	r_o*	a	W	r_i*†	a_i†	$R_{Coulomb}$	Ref. No.
	(Mev)	(fm)	(fm)	(MeV)	(fm)	(fm)	(fm)	
$^{14}_{N} + ^{12}_{C}$	97.68	1.07	.519	$2.95 + .45E_{cm}$	1.40	.519	1.07	This work
$^{14}_{N} + ^{12}_{C}$	14.0	1.35	.35	$.4 + .1\ E_{cm}$	1.40	.35	1.40	10
$^{12}_{C} + ^{13}_{C}$	100.0	1.36	.48	15.0	1.43	.26	1.36	11
$^{16}_{0} + ^{14}_{N}$	7.5	1.35	.49	$.4 + .15E_{cm}$	1.35	.49	1.35	12
$^{16}_{0} + ^{15}_{N}$	7.5	1.35	.49	$.4 + .15E_{cm}$	1.35	.49	1.35	12
$^{16}_{0} + ^{16}_{0}$	12.0	1.35	.49	$.4 + .15E_{cm}$	1.35	.49	1.35	12
$^{16}_{0} + ^{18}_{0}$	17.0	1.35	.49	$.4 + .15E_{cm}$	1.35	.49	1.35	12
$^{16}_{0} + ^{16}_{0}$	17.0	1.35	.49	$.4 + .01E_{cm}$	1.35	.49	1.35	13
$^{16}_{0} + ^{16}_{0}$	17.0	1.35	.49	$.8 + .2\ E_{cm}$	1.26	.15	1.35	13
$^{14}_{N} + ^{14}_{N}$	15.0	1.35	.49	$.4 + .13E_{cm}$	1.35	.49	1.35	13
$^{12}_{C} + ^{12}_{C}$	14.0	1.35	.35	$.4 + .1\ E_{cm}$	1.40	.35	1.35	13

*$R_o = r_o(A_t^{1/3} + A_p^{1/3})$

†For the four parameter optical model $r_i = r_o$

$a_i = a$

Table I. Optical-model parameters for elastic scattering of nuclei in mass region A ≈ 16.

parameters used to describe similar data from nuclei in the same mass region. It is well known that elastic scattering is only sensitive to the surface region of the potential and therefore, optical model parameter sets which satisfy the equations

$$V \cdot \exp(R_o/a) = \text{constant}$$
$$W \cdot \exp(R_o/a) = \text{constant}$$

yield equivalent fits to the data. This is sometimes referred to as the Igo ambiguity[14]. The constant for the $^{14}N + ^{12}C$ parameters reported by Hanson, et al.,[15] is 663, while the constant derived from our parameters is 5863. Clearly, this does not alone account for the discrepancy. Another important ambiguity is known as the phase equivalent discrete ambiguity[16]. For the same geometrical parameters, potential depths of different discrete values yield the identical calculated cross sections. This arises when potentials of different depths produce a different number of nodes in the interior wave function. Since the elastic scattering cross section is insensitive to the interior region of the potential, these discrete potentials yield identical scattering cross sections. Together these two ambiguities may explain the large differences between the parameter sets. Using the Hanson parameters to fit our 21.0 MeV angular distribution lead to a χ^2 deviation of 1950, a relatively poor fit. The explanation for this discrepancy could be that while our parameters give a better fit over the laboratory energy range 15.0 to 25 MeV, when one considers a larger energy range, the fit over the 15 to 25 MeV energy range has to be sacrificed. As an example of this, in Figure 11, $^{16}O + ^{16}O$ excitation

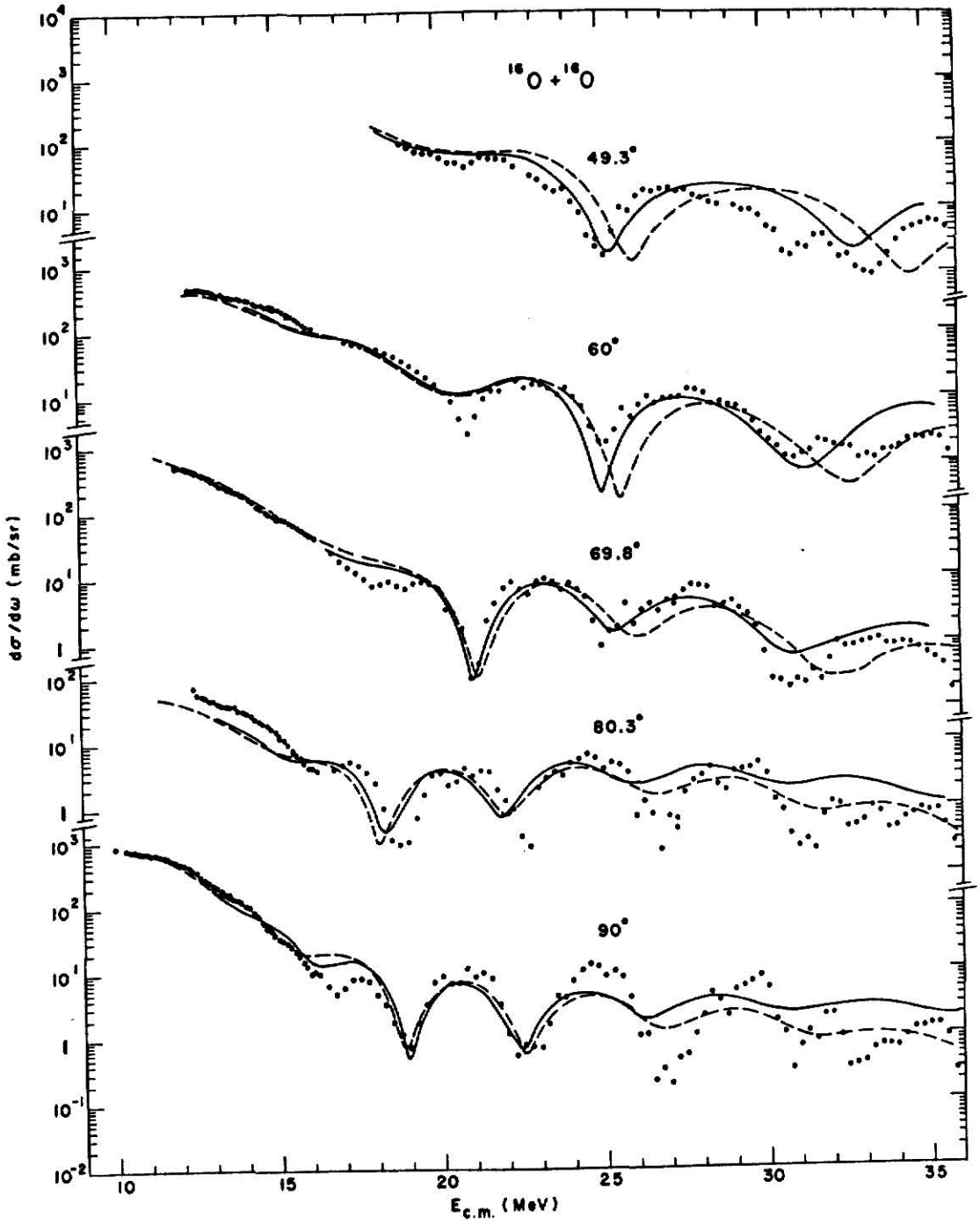

Reference Proc. Sym. Heavy-Ion Scattering, Argonne, 1971 (Argonne Nat. Laboratory, Argonne, Illinois, 1973), 173.

Figure 11. Comparison between the $^{16}O + ^{16}O$ excitation functions and the optical model calculations with energy-dependent (solid curves) and energy-independent (dashed curves) real potential.

functions are fitted by the optical model[17]; it may be possible that if one considered a smaller energy range he could obtain a better fit with different parameters.

In Ref. 10, the authors obtain the parameters for $^{14}N + ^{12}C$ from an article by Reilly et al.[18], but in Reilly's article only the identical nuclei optical model parameters are given. It is possible that Hanson obtained the parameters from those for the $^{14}N + ^{14}N$ and $^{12}C + ^{12}C$. If this is the case, then our results cast doubt on the validity of this assumption.

B. Optical Model and Excitation Functions

We first used the parameters that gave the best average description to all three angular distributions. We obtained fairly good fits except for the most backward angle excitation functions. In an attempt to better fit these backward angles, we tried to use an imaginary potential which varied with energy. By assuming a linear variation of W between the best fit values at 20.0 and 23.5 MeV, we obtained for W the equation $W = 2.95 + .207\ E_{lab}$. This gave the best fit to the measured cross sections. Figures 5, 6 and 7 compare the experimental excitation functions to the optical model calculation. A few typical error bars are included.

The error bars were derived from the statistical counting error, $\sigma/\sigma_R \cdot \sqrt{Y}$, and the experimental error. The experimental error, .021 σ/σ_R, was obtained from a .5% error associated with the current integrater, a 1% error assumed for the ADC and a 1.8% error that was derived by taking two excitation functions, each measured independently

at $\Theta_{cm} = 70°$. This 1.8% error is an indication of the reproducibility of the measured excitation functions. The total error is then given by the square root of the sum of their squares. At the forward angles the experimental error dominates and at the background angles the statistical errors dominate.

It is surprising that when comparing our excitation functions to those of the identical nuclei, Figure 11, the overall shape is similar to the $^{14}N + ^{14}N$ excitation function while it has very little resemblance to the $^{12}C + ^{12}C$ excitation function. The smooth gross structure indicates that resonances, as found in $^{12}C + ^{13}C$, in the same energy range, do not exist for $^{14}N + ^{12}C$. This is in agreement with a recent article by H. L. Hanson and associates.[19] They predict that there will be no resonances observed in the $^{14}N + ^{12}C$ elastic scattering cross section or reaction cross sections. Also, as reported by Voit, et al.,[20] the excitation functions for the $^{14}N + ^{12}C$ alpha and proton channels, as seen in Figure 13, exhibit little structure which indicates a lack of any resonances in this energy region.

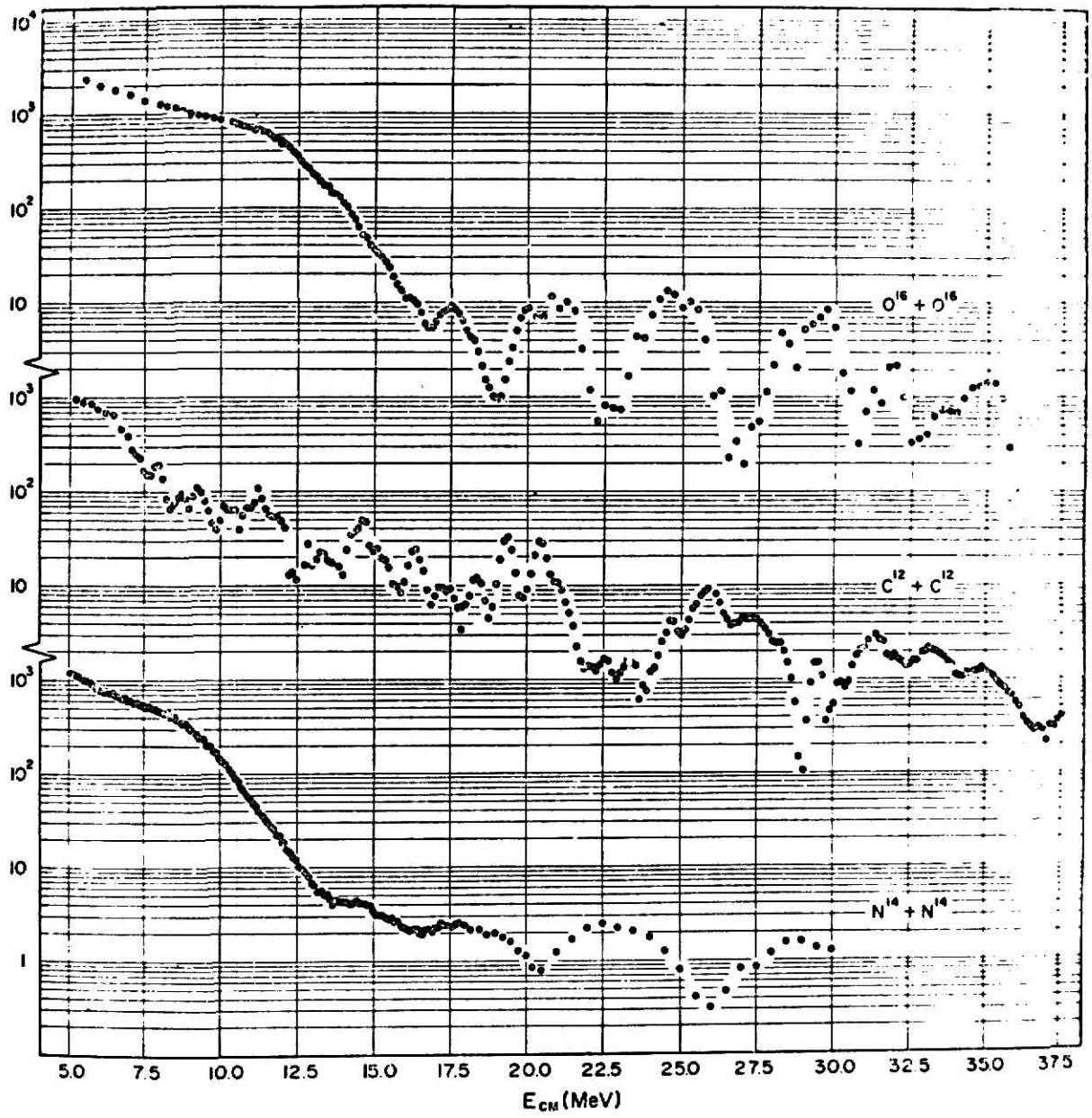

Reference W. Reilly, R. Weiland, A. Gobbi, M. W. Sachs and D. A. Bromley, Nuovo Cimento 13A, 903 (1973).

Figure 12. Comparison of the $\theta_{cm} = 90^{o}$ elastic scattering excitation functions for the identical nuclei $^{16}O + ^{16}O$, $^{12}C + ^{12}C$ and $^{14}N + ^{14}N$ reactions.

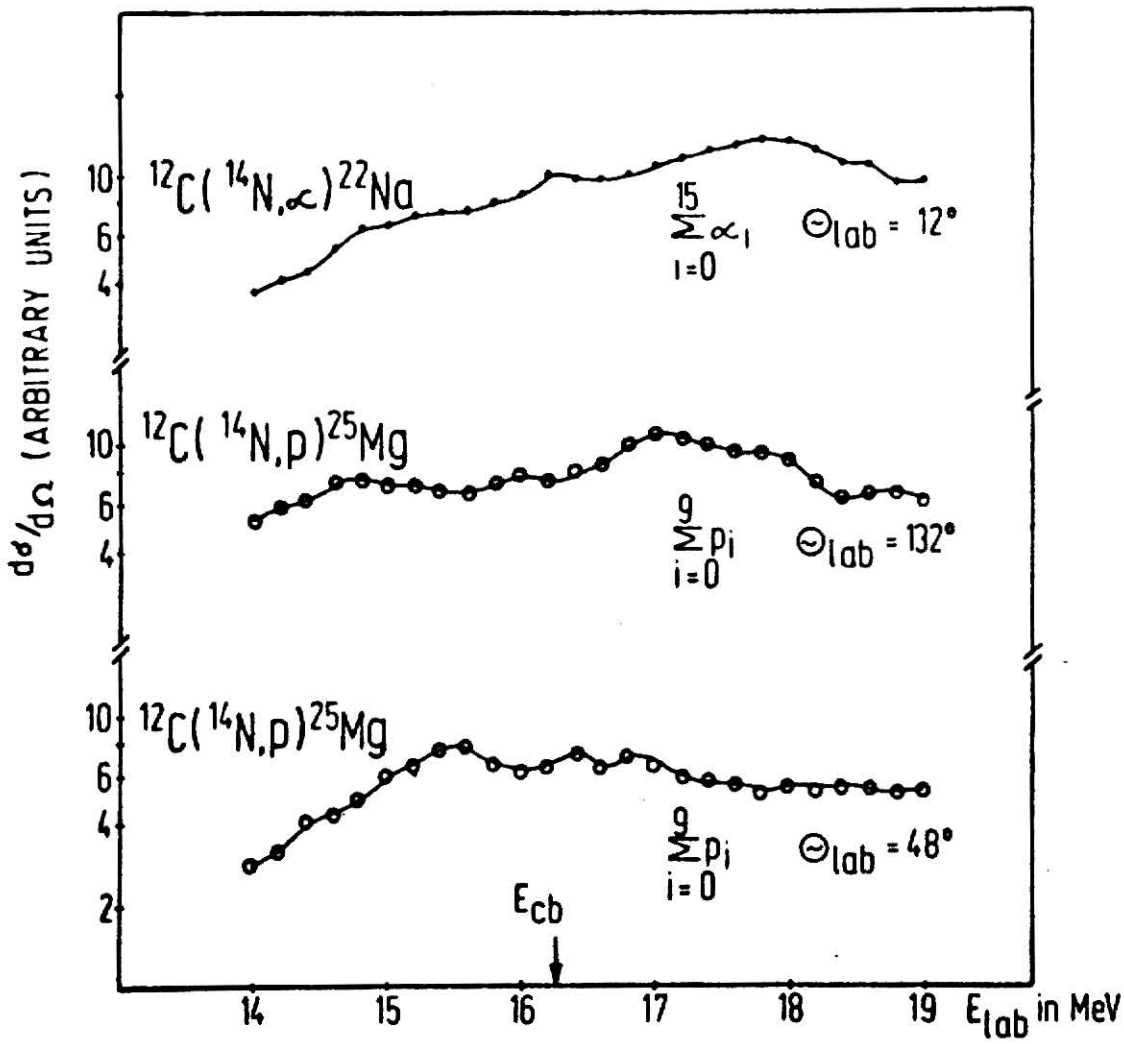

Reference H. Voit, G. Ischenko, F. Siller and H. D. Helb, Nuc. Phys., A179, 29 (1972).

Figure 13. Excitation functions for the $^{14}N + ^{12}C$ alpha and proton channels.

V. CONCLUSION

> The shrewd guess, the fertile hypothesis, the courageous leap to a tentative conclusion--these are the most valuable coin of the thinker at work. But in most schools guessing is heavily penalized and is associated somehow with laziness
>
> Jerome Seymour Bruner
> The Process of Education

We have found that in the laboratory energy range 15 to 24.8 MeV the elastic scattering excitation functions of $^{14}N + ^{12}C$ have an overall shape like those of $^{14}N + ^{14}N$ and are characterized by a smooth variation with energy. Because only smooth gross structures were observed, the prediction that resonances do not exist in this reaction is in agreement with our results. We do not have this same agreement with the optical model parameters published by Hanson et al. Over the laboratory energy region studied our parameters gave a distinctly better fit. Due to this and the statement; "Insofar as possible, they (optical model parameters) are obtained from analyses of elastic scattering data"[18] we feel that the parameters presented by Hanson et al. were an invalid average of those of $^{14}N + ^{14}N$ and $^{12}C + ^{12}C$. This demonstrates the worth of experiments of this type and the need for more optical model studies.

With the need for more optical model studies, the lessons of this experiment become important. Improvements on the Faraday cup monitoring method, the gold monitoring technique, the computer codes developed,

the useful formula for the average charge state of nitrogen in solids and the method for obtaining such formulas will all improve optical model studies.

Because of the relative ease of performing this experiment and the knowledge obtained, we believe that elastic scattering studies are one of the most efficient methods of studying the nucleus. With the computer codes written and the experimental methods established, we are in a position where it is possible to study large numbers of nuclear elastic scattering reactions and to parameterize these reactions by the optical model parameters. By studying the trends in these reactions we can derive theories to explain the different shapes of the elastic scattering cross sections, predict resonances, and predict optical model parameters for still more nuclear scattering reactions. And with successful prediction comes scientific understanding.

REFERENCES

1. W. Reilly, R. Weiland, A. Gobbi, M. W. Sachs and D. A. Bromely, Nuovo Cimento 13A, 903 (1973).
2. See Ref. 1, 911.
3. J. C. Legg, private communication.
4. D. L. Hanson, R. G. Stokstod, K. A. Erb, C. Olmer, M. W. Sachs and D. A. Bromely, Phys. Rev. 9C, 1760 (1974).
5. D. L. Hanson, R. G. Stokstod, K. A. Erb, C. Olmer and D. A. Bromely, Phys, Rev. 9C, 930 (1974).
6. E. J. Feldl, P. B. Weiss and R. H. Davis, Nuc. Inst. and Met. 28, 309 (1964).
7. J. B. Marion and F. C. Young, Nuclear Reaction Analysis Graphs and Tables, (North-Holland Publishing Company, Amsterdam, 1963), 42.
8. R. J. Eastgate, W. J. Thompson, R. A. Hardekopf, Comp. Phys. Comm. 5, 69-74 (1973), and W. J. Thompson, private communication.
9. H. G. Bohlen, M. Feil, A. Gamp, B. Kohlmeyer, N. Marguardt, W. von Oertzen, Phys. Letl. 41B, 425-428 (1972).
10. See Ref. 5, 930.
11. See Ref. 9.
12. Proc. Sym. Heavy-Ion Scattering, Argonne, 1971 (Argonne Nat. Laboratory, Argonne, Illinois, 1971), 164.
13. See Ref. 1, 897.
14. W. J. Thompson, G. E. Crawford and R. H. Davis, Nuc. Phys. A98, 228-240 (1967), and W. J. Thompson, private communication.
15. See Ref. 5, 930.

16. John S. Eck, Phys. Rev. 3C, 949-952 (1971), and private communication.

17. See Ref. 12, 173.

18. See Ref. 1, 912.

19. See Ref. 4, and W. J. Thompson, private communication.

20. H. Voit, G. Ischenko, F. Siller and H. D. Helb, Nuc. Phys. A179, 29 (1972).

ACKNOWLEDGEMENTS

The author wishes to acknowledge the advice and assistance of the many people who made this project possible.

Dr. John S. Eck, my major professor.

Dr. Basil Curnutte and Dr. Hulan Jack, my committee members.

Donald O. Elliott, Keith A. Jamison and Steven A. Schiller, my friends and colleagues.

Rachel Johnson, my wife.

The Atomic Energy Commission is also to be acknowledged for the sponsoring of this research.

STUDY OF THE ELASTIC SCATTERING OF ^{14}N ON ^{12}C

by

JAMES H. JOHNSON

B.A., University of Northern Colorado, 1972

An abstract of A MASTER'S THESIS

submitted in partial fulfillment of the

requirements for the degree

MASTER OF SCIENCE

Department of Physics

KANSAS STATE UNIVERSITY
Manhattan, Kansas

1974

ABSTRACT

The elastic scattering of ^{14}N from ^{12}C has been studied in the laboratory energy region 15 to 25 MeV. Angular distributions have been measured using a thick (40 $\mu g/cm^2$) target for lab energies 20.0, 21.0 and 23.5 MeV. Excitation function measurements were taken at Θ_{lab} = 25°, 35°, 45° and 55° using both a thick (40 $\mu g/cm^2$) and thin (10 $\mu g/cm^2$) targets. The optical model parameters that best describe the elastic scattering cross section were found and were compared to other parameter sets for similar reactions in the same mass region (A ≃ 16). From the results there is no indication that resonances exist in this reaction. The general shape of $^{14}N + ^{12}C$ excitation function is found to be similar to the $^{14}N + ^{14}N$ excitation function, while it has little resemblance to the $^{12}C + ^{12}C$ excitation function.